

Spectral properties of thermal fluctuations on simple liquid surfaces below shot-noise levels

Kenichiro Aoki* and Takahisa Mitsui†

Research and Education Center for Natural Sciences and Department of Physics, Hiyoshi, Keio University, Yokohama 223-8521, Japan

(Received 13 December 2011; published 18 July 2012)

We study the spectral properties of thermal fluctuations on simple liquid surfaces, sometimes called ripples. Analytical properties of the spectral function are investigated and are shown to be composed of regions with simple analytic behavior with respect to the frequency or the wave number. The derived expressions are compared to spectral measurements performed orders of magnitude below shot-noise levels, which is achieved using a novel noise reduction method. The agreement between the theory of thermal surface fluctuations and the experiment is found to be excellent, elucidating the spectral properties of the surface fluctuations. The measurement method requires relatively only a small sample both spatially (few μm) and temporally (~ 20 s). The method also requires relatively weak light power (~ 0.5 mW) so that it has a broad range of applicability, including local measurements, investigations of time-dependent phenomena, and noninvasive measurements.

DOI: [10.1103/PhysRevE.86.011602](https://doi.org/10.1103/PhysRevE.86.011602)

PACS number(s): 68.03.Kn, 05.40.-a, 66.20.-d

I. INTRODUCTION

Thermal fluctuations are ubiquitous. While usually not noticed, all types of surfaces, solid, liquid or otherwise, are fluctuating thermally. However, the fluctuations tend to be too small to be observed or measured directly, except under special circumstances. Indirectly, the fluctuations can be visible through phenomena such as Brownian motion and thermal noise in electronic circuits, referred to as Johnson-Nyquist noise. Phenomena in which thermal fluctuations can be examined directly in nonexotic materials are surface fluctuations of liquids, sometimes called “ripples” [1]. Using surface light scattering, thermal surface and interface fluctuations of liquids have been studied for some time [2] and are of current experimental, as well as theoretical interest [3–8]. Other direct thermal fluctuation measurements include high power interferometry of mirror surfaces [9] and fluctuations of surfaces with exceptionally low surface tension [10].

In this work, we detect reflected light from surfaces to measure their inclination spectra [11–13]. Essentially, the sample surface acts partially as a mirror and its inclination can be obtained regarding it as an optical lever [14]. The dynamical measurements can be Fourier transformed to obtain the inclination fluctuation spectra of surfaces. While we concentrate on thermal surface fluctuations of simple liquids in this work, our method has a much broader applicability in studying surface and interface fluctuation spectra, some of which was explored in [13]. Our measurements are somewhat complementary to the more traditional spectral measurements performed at specific wavelengths [2, 15–20]. Compared to the standard surface light scattering methods, the approach can be characterized more as a surface light *reflection* measurement, wherein almost all the light reflected by the surface is collected. Consequently, our measurements require less power than the traditional scattering methods and requires less time (typically around 20 s for obtaining a spectrum shown below). The measurement also affects the sample less since lower power is applied for a shorter period of time, which can be crucial

when noninvasiveness is required. The short measurement time allows the method to be used to investigate dynamical changes in the spectra. Furthermore, we do not require that the surface act as effective gratings so that the measurements can be performed on smaller samples, rough surfaces, and highly viscous fluids with strong dissipation. Since we focus the beam, a particular region in depth can be selected so that the method can be used in the studies of interface phenomena as well. As explained below, it is possible to independently calibrate the magnitude of the fluctuations we measure, which seems difficult in the more traditional scattering experiments. The measurement system can be made simpler than the surface light scattering approach.

While shot noise is often regarded as an unavoidable limitation in optical measurements, we show that such is not the case. The measurements involve novel methods that allow us to measure the spectrum directly, down to several orders of magnitude below the shot-noise level. Intuitively speaking, by using the correlation of two independent measurements of the same signal, we eliminate the noise, which is decorrelated. As we explain, this principle is not limited to thermal noise measurements nor to surface light scattering measurements. The experimental results agree with the theory quite well. In the process, we elucidate the simple analytic behavior of the spectra and show how it appears in the full spectrum, which can be seen in experiments.

The dispersion relation for surface waves on a simple liquid surface can be derived from the Navier-Stokes equation, when the viscosity of the liquid can be ignored, as [21]

$$\omega(k) = \sqrt{\frac{\sigma k^3}{\rho} + gk}. \quad (1)$$

Here, g is the gravitational acceleration, ρ, σ are the density and the surface tension of the liquid, k is the wave number, and ω is the (angular) frequency. The viscosity becomes more important for shorter wavelengths and dissipation will play an essential role below. Gravitational effects are more important for longer wavelengths but are negligible for wavelengths much smaller than $\pi\sqrt{\sigma/(\rho g)}$. For liquids we examine, namely, water, ethanol, and oil, gravitational effects are unimportant for scales below 10 mm. The samples we

*ken@phys-h.keio.ac.jp

†mitsui@phys-h.keio.ac.jp.

examine have surface sizes of few mm and longer wavelengths are effectively cut off, so that henceforth we ignore effects due to gravity. Under these circumstances, the dispersion relation reduces to the following two equivalent relationships.

$$\omega = \omega_R(k) = \sqrt{\frac{\sigma k^3}{\rho}}, \quad k = k_R(\omega) = \left(\frac{\rho \omega^2}{\sigma}\right)^{1/3}. \quad (2)$$

While the beam size that determines the observed surface region is much smaller than the sample size, the inclinations of waves with wavelengths much larger than the beam size can still be measured. In addition to the cutoff due to the sample size, there is an additional cutoff for shorter wavelengths to be explained below. Intuitively speaking, since the average inclination within the beam spot is measured, shorter wavelengths are averaged out. In what follows, we examine the spectra of surface fluctuations within these cutoffs, both experimentally and theoretically, including the full effects of dissipation.

The paper is organized as follows: In Sec. II, we explain the surface light reflection experiment and derive what precisely is measured by this method. The properties of thermal surface fluctuations of simple liquids are examined in Sec. III and the approximate simple analytic behavior of the spectra are derived. The shot-noise level in our experiments are assessed in Sec. IV. The noise reduction method explained in Sec. V allows us to detect weak signals buried under the shot-noise level. The general applicability of the principle is also clarified. Finally, we combine the theoretical and the experimental results in Sec. VI and find that they agree. The limitations in the experiment and further directions for research are also discussed.

II. THE EXPERIMENT AND THE MEASUREMENT

In the experiment, a laser beam is shone on the sample and the average inclination within the beam spot is measured at each instant (Fig. 1). The surface effectively acts as an optical lever [14] and its inclination can be measured through the difference in the amount of light received by each element in a dual-element photodiode (DEPD 1,2, S4204 Hamamatsu Photonics, Japan). We use two such independent measurement systems with a laser beam 1 (wavelength 638 nm) and 2 (658 nm). The reason for using these two systems is to reduce unwanted noise in the measurements, which we achieve by using correlations of two independent measurements, since the noise within them is decorrelated. The principle behind this noise reduction is described in Sec. V in detail. The DEP signals are amplified and then fed into a computer via analog to digital converters (ADC, 14 bit, ADXII14-80M, Saya, Japan). The inclination data in the time domain are converted to the spectral information through the use of Fourier transform. Fourier transforms and averagings are performed by the computer.

The total laser beam power at the sample is 0.5 mW. The beam is focused down to μm order and its diameter ($\sim \lambda/\text{NA}$) is varied by changing the numerical aperture (NA) of the objective lens, where λ is the wavelength of the probe laser beam. This focusing allows us to select a particular region of interest in the depth direction, which can, for instance, be useful in the studies of interface phenomena. The beam size is considerably smaller than that used in the standard light

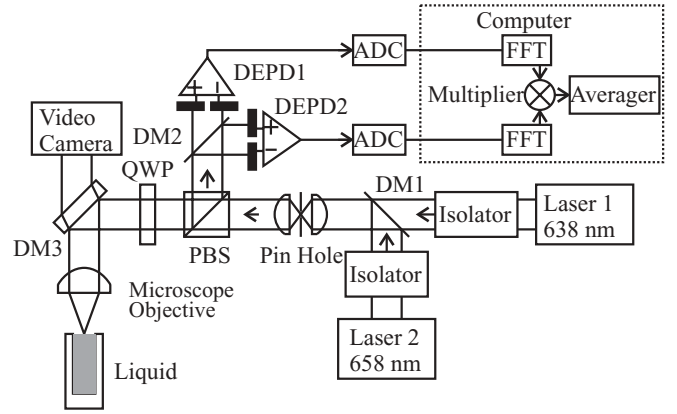


FIG. 1. Two laser beams with wavelengths 638 and 658 nm are combined at a dichroic mirror (DM1) and focused by a microscope objective lens onto the liquid surface. The reflected light with different wavelengths are separated at DM2 to obtain two independent inclination measurements of the same surface. The inclination is converted into electric signals using DEP1, DEP2 and are fed via ADCs into a computer where fast Fourier transform (FFT) and averagings are performed. A polarizing beam splitter (PBS) and a quarter wave plate (QWP) are included to extract the light reflected back from the sample efficiently. DM3 is used for viewing the sample through a video camera.

scattering methods. The amplitude of the waves are small compared to the wavelength so that the reflected light is almost all collected by the objective lens. Therefore, compared to the standard light scattering experiments which observe only a small fraction of the scattered light, we obtain larger signals for a given beam power. This can be crucial in low power measurements.

We now explain what is measured in this experiment and how this relates to the spectrum of surface fluctuations. Since the surface acts effectively as an optical lever, we measure fluctuations in the average inclination of the surface. The average inclination can be obtained by approximating the surface level, $\phi(\mathbf{r}, t)$, with a linear profile. This can be done by minimizing

$$\int d^2\mathbf{r} G(\mathbf{r}) |\phi(\mathbf{r}, t) - (a_0(t) + a_1(t)x)|^2. \quad (3)$$

Here, $\mathbf{r} = (x, y)$ are coordinates on the surface and $G(\mathbf{r})$ is the beam profile function. In what follows, the results from this approach are thoroughly compared with the experimental results on various liquids, with which they agree quite well. Equation (3) leads to the expression for the average displacement a_0 and inclination a_1 ,

$$a_0(t) = C_0 \int d^2\mathbf{r} G(\mathbf{r}) \phi(\mathbf{r}, t), \quad C_0 = \left(\int d^2\mathbf{r} G(\mathbf{r}) \right)^{-1}, \quad (4)$$

$$a_1(t) = C_1 \int d^2\mathbf{r} G(\mathbf{r}) x \phi(\mathbf{r}, t), \quad C_1 = \left(\int d^2\mathbf{r} x^2 G(\mathbf{r}) \right)^{-1}. \quad (5)$$

While we can solve for $a_j(t)$ more generally, we assumed here that the profile is symmetric, $\int d^2\mathbf{r} x G(\mathbf{r}) = 0$, which

applies to our case, as discussed below. We define the Fourier transform of a_j as

$$\tilde{a}_j(\omega) = \frac{1}{\sqrt{T}} \int_{-T/2}^{T/2} dt e^{i\omega t} a_j(t), \quad j = 1, 2, \quad (6)$$

where T is the measurement time, which is much longer when compared to the other time scales involved.

Since the correlation function of the surface fluctuations is translation invariant both in space and time, it can be expressed as

$$\langle \phi(\mathbf{r}, t) \phi(\mathbf{r}', t') \rangle = \int d\omega \int \frac{d^2\mathbf{k}}{(2\pi)^2} e^{i\mathbf{k}\cdot(\mathbf{r}-\mathbf{r}') - i\omega(t-t')} P(k, \omega). \quad (7)$$

Here, $P(k, \omega)$ is the spectral function of the fluctuations of the surface displacement and $\langle \dots \rangle$ denotes the statistical average. Using this correlation function, the fluctuations in the inclinations are obtained as

$$\langle |\tilde{a}_1(\omega)|^2 \rangle = \int \frac{d^2\mathbf{k}}{2\pi} \left| C_1 \int d^2\mathbf{r} e^{i\mathbf{k}\cdot\mathbf{r}} x G(\mathbf{r}) \right|^2 P(k, \omega). \quad (8)$$

Since we are using a laser beam well described by a Gaussian profile to observe surface fluctuations, the profile function $G(\mathbf{r})$ can be expressed using the beam diameter b as

$$G(\mathbf{r}) = G_0 e^{-4r^2/b^2}. \quad (9)$$

The spectrum measured in the experiment is (we henceforth use the notation $\omega = 2\pi f$)

$$S(f) = 2 \langle |\tilde{a}_1(\omega)|^2 \rangle, \quad (10)$$

taking into account that the measurement is in frequency space and the one-sidedness of the spectrum. Combining the results above, we derive a compact expression for the fluctuation spectrum observed in the experiment,

$$S(f) = \int_0^\infty dk k^3 e^{-b^2 k^2/8} P(k, 2\pi f). \quad (11)$$

It should be noted that this formula applies to general surface fluctuation spectra measured using this method and is not limited to liquids nor to thermal fluctuations. This result specifies the measured spectrum $S(f)$ *completely* including its magnitude, given the spectral function $P(k, \omega)$ and the beam diameter b , and is independent of the beam power applied. As can be seen from the expression, the role of the beam size is to effectively cut off the k integral of the spectral functions for values over $\sim 2\pi/b$. Consequently, fluctuations with wavelengths much smaller than the probe light wavelength cannot be investigated using this method, which is a general limitation of optical measurements, unless we use near-field methods. This cutoff occurs because the inclination is effectively averaged within the beam spot, so that shorter wavelengths are effectively averaged out. It also explains why we integrate up to infinity in this formula; while, in principle, the wavelengths of surface fluctuations should be cutoff at atomic length scales, this is much smaller than b so that using infinity as the upper limit in the integration

region introduces negligible difference, due to the Gaussian damping. The lower limit of the integration region should, strictly speaking, be set to $\sim 2\pi/L$, where L is the size of the sample (L is few mm in our experiment) providing an upper bound for wavelengths. However, the difference from setting the lower end of the integral to zero as in the formula can also be ignored, as will become clear below.

III. ANALYTIC STRUCTURE OF THE SPECTRUM

The spectral function for thermal fluctuations of simple liquid surfaces has been derived previously [22],

$$P(k, \omega) = \frac{k_B T}{\pi} \frac{k u^2}{\rho \omega^3} \text{Im}[(1 - iu)^2 + y - \sqrt{1 - 2iu}]^{-1}, \quad (12)$$

$$u \equiv \frac{\rho \omega}{2\eta k^2} \quad y \equiv \frac{\rho \sigma}{4\eta^2 k}.$$

While this expression for the spectrum is analytic, its dependence on the various physical parameters is not apparent. The dependence can be obtained in simple form when the wave number domain or the frequency domain is split into several regimes, depending on the viscosity. We concisely summarize this dependence below, to gain insight into the behavior of the spectral function and for later use.

A. Leading analytic behavior with respect to k

Let us study the dependence of the spectral function $P(k, \omega)$ on k , when ω is fixed. The dimensionless measure of the viscosity of the liquid, $\eta^3 \omega / (\rho \sigma^2)$ influences the properties of the spectral function $P(k, \omega)$ qualitatively. Any liquid is highly dissipative for high enough frequencies, which is intuitively natural. When the viscosity is effectively low, $\eta^3 \omega / (\rho \sigma^2) < 1/(8\sqrt{2})$, the leading order analytic behavior $P_0(k, \omega)$ can be obtained as

$$P_0(k, \omega) = \frac{k_B T}{\pi} \times \begin{cases} \frac{4\eta k^3}{\rho^2 \omega^4} & \text{when } k < 2^{-1/6} k_R(\omega) \\ \frac{2\eta}{\sigma^2 k^3} & k > 2^{-1/6} k_R(\omega) \end{cases}. \quad (13)$$

In this case, $P(k, \omega)$ has a peak close to $k = k_R(\omega)$, which becomes less prominent as $\eta^3 \omega / (\rho \sigma^2)$ increases. When $\eta^3 \omega / (\rho \sigma^2) > 1/(8\sqrt{2})$, the leading behavior of the dispersion relation splits into three regions as

$$P_0(k, \omega) = \frac{k_B T}{\pi} \times \begin{cases} \frac{4\eta k^3}{\rho^2 \omega^4} & \text{when } k < 2^{-1/4} \sqrt{\frac{\rho \omega}{2\eta}} \\ \frac{1}{2\eta k \omega^2} & 2^{-1/4} \sqrt{\frac{\rho \omega}{2\eta}} < k < \frac{2\eta \omega}{\sigma} \\ \frac{2\eta}{\sigma^2 k^3} & k > \frac{2\eta \omega}{\sigma} \end{cases}. \quad (14)$$

In both cases with low and high viscosity, for long wavelengths compared to $2\pi/k_R(\omega)$, the spectral function is governed by the viscous properties of the liquid and depends on ρ . On the other hand, for short wavelengths, it is suppressed by the surface tension of the liquid and is independent of its density.

In Fig. 2, we compare the full spectral function Eq. (12) with its approximate analytic behavior derived above. We see that in all the cases, the spectrum is well reproduced by them, except

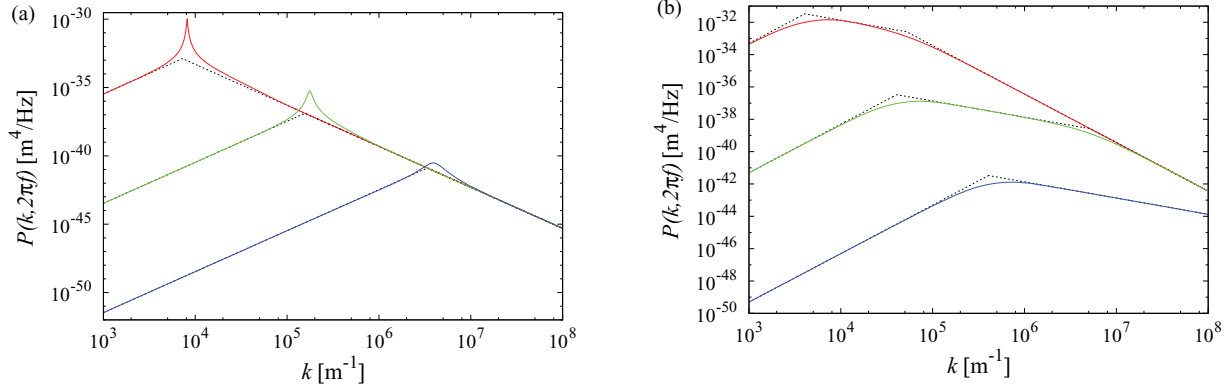


FIG. 2. (Color online) $P(k, 2\pi f)$ computed numerically for (a) water and (b) oil with respect to k at fixed f . Frequencies are $f = 10^3, 10^5, 10^7$ (s^{-1}) [red (upper), green (middle), blue (lower) lines, respectively], with the maximum of the spectrum being larger for higher f . The corresponding simple analytic behaviors Eqs. (13) and (14) are also shown (black dashed) and match well with the full spectral function and are almost invisible, except at the boundaries between the regions.

for the peak seen in the water surface fluctuations at lower frequencies. The peak reflects long-lived waves and disappears when the viscosity is effectively high, due to dissipation. In both Eqs. (13) and (14), the spectral function is independent of f for large k , which can be seen from the plots. The simple analytic formulas derived above capture the situations with weak and strong viscosity, which have qualitatively different properties.

B. Leading analytic behavior with respect to ω

We now analyze the dependence of $P(k, \omega)$ on ω , for fixed k (Fig. 3). For a liquid with low viscosity effectively, $\eta^2 k / (\rho \sigma) < 1/(4\sqrt{2})$, the leading order analytic behavior $P_0(k, \omega)$ is broken up into two regions as

$$P_0(k, \omega) = \frac{k_B T}{\pi} \times \begin{cases} \frac{2\eta}{\sigma^2 k^3} & \text{when } \omega < 2^{1/4} \omega_R(k) \\ \frac{4\eta k^3}{\rho^2 \omega^4} & \omega > 2^{1/4} \omega_R(k) \end{cases}. \quad (15)$$

For the highly viscous case, the leading analytic behavior can be broken down into three regions, thus,

$$P_0(k, \omega) = \frac{k_B T}{\pi} \times \begin{cases} \frac{2\eta}{\sigma^2 k^3} & \text{when } \omega < \frac{\sigma k}{2\eta} \\ \frac{1}{2\eta k \omega^2} & \frac{\sigma k}{2\eta} < \omega < \frac{2\sqrt{2}\eta k^2}{\rho} \\ \frac{4\eta k^3}{\rho^2 \omega^4} & \omega > \frac{2\sqrt{2}\eta k^2}{\rho} \end{cases}. \quad (16)$$

C. Analytic behavior of the integrated spectrum

While the spectrum $S(f)$ in Eq. (11) can be computed numerically, we now clarify its rough analytic behavior using $P_0(k, 2\pi f)$ derived above. In the integrated spectrum $S(f)$, b provides a cutoff k_{\max} for the integral, whose relation we specify below. The spectrum can be approximated by

$$S_0(f) = \int_0^{k_{\max}} dk k^3 P_0(k, 2\pi f). \quad (17)$$

This can be computed explicitly. For the low viscosity case $\eta^3 \omega / (\rho \sigma^2) < 1/(8\sqrt{2})$,

$$S_0(f) = \frac{k_B T}{\pi} \times \begin{cases} \left(\frac{2\eta k_{\max}}{\sigma^2} - \frac{2^{11/6} 3 \rho^{1/3} \eta}{7 \sigma^{7/3}} \omega^{2/3} \right) & \text{when } \omega < 2^{1/4} \omega_R(k_{\max}) \\ \frac{4\eta k_{\max}^7}{7 \rho^2} \frac{1}{\omega^4} & \omega > 2^{1/4} \omega_R(k_{\max}) \end{cases}. \quad (18)$$

When the viscosity is high, the spectrum has the following approximate:

$$S_0(f) = \frac{k_B T}{\pi} \times \begin{cases} \left(\frac{2\eta k_{\max}}{\sigma^2} - \frac{8\eta^2}{3\sigma^3} \omega - \frac{\rho^{3/2}}{2^{5/4} 21 \eta^{5/2}} \frac{1}{\omega^{1/2}} \right) & \text{when } \omega < \frac{\sigma k_{\max}}{2\eta} \\ \left(\frac{k_{\max}^3}{6\eta} \frac{1}{\omega^2} - \frac{\rho^{3/2}}{2^{5/4} 21 \eta^{5/2}} \frac{1}{\omega^{1/2}} \right) & \frac{\sigma k_{\max}}{2\eta} < \omega < \frac{2\sqrt{2}\eta k_{\max}^2}{\rho} \\ \frac{4\eta k_{\max}^7}{7 \rho^2} \frac{1}{\omega^4} & \omega > \frac{2\sqrt{2}\eta k_{\max}^2}{\rho} \end{cases}. \quad (19)$$

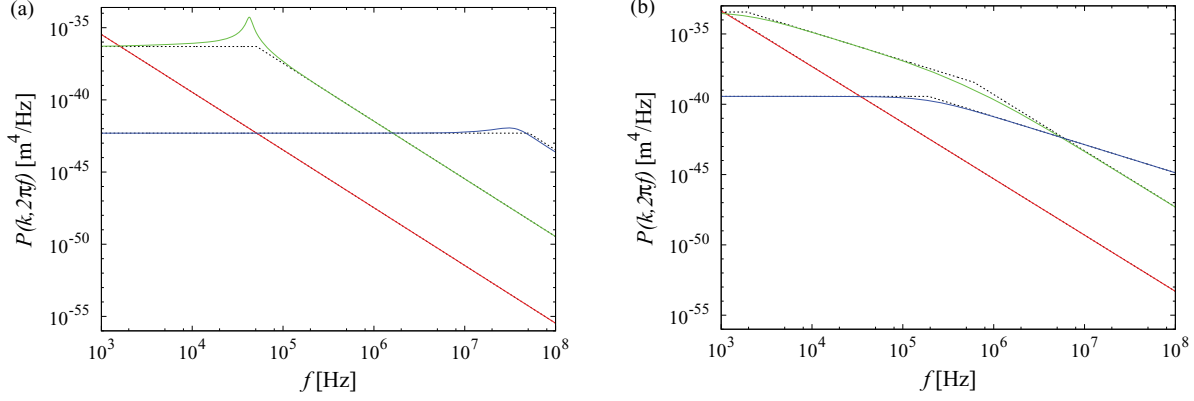


FIG. 3. (Color online) $P(k, 2\pi f)$ obtained numerically for (a) water and (b) oil with respect to frequency f at $k = 10^3, 10^5, 10^7$ (m^{-1}) [red (smallest at highest frequencies), green and blue (largest at highest frequencies) lines, respectively]. The spectra with larger k have more fluctuations at higher f . Their analytic approximations Eqs. (15) and (16) (black dashed) agree well with the full spectral function and are almost invisible, except at the boundaries between the regions.

Taking into account the formula for $S(f)$ in Eq. (11), we use $k_{\text{max}} = 2^{1/4}4/b$, which satisfies $\int_0^\infty dk \exp(-b^2 k^2/16) k^3 = \int_0^{k_{\text{max}}} dk k^3$. In Fig. 4, the spectrum $S(f)$ is compared to its approximate analytic behavior $S_0(f)$ in Eqs. (18) and (19). It can be seen that the essential features of $S(f)$ are well reproduced by the simple analytic formulas. Examining in more detail, we see that the agreement is better for more viscous liquids. This is presumably due to the peak contribution unaccounted for in the formulas Eqs. (13) and (14), which does not exist for more viscous fluids. It can be seen from Eqs. (18) and (19) that $S(f)$ behaves as $\sim \eta/\sigma^2$ for lower frequencies explaining why oil has larger fluctuations than water in this regime. In addition, from the formulas we can see why the fluctuations are larger for smaller b (or equivalently, larger k_{max}) over the whole spectrum, both when the viscosity is weak and strong.

We note that the calculations above also show why the integration region in the spectrum formula Eq. (11) can be taken down to zero as long as the cutoff is well below the upper limit of the region; since had we put in a lower cutoff k_{low} , its contribution to $S(f)$ would behave as $\sim k_{\text{low}}^7$. This condition is

equivalent to the surface size being much larger than the beam diameter, which is always satisfied in our experiments.

IV. SHOT-NOISE LEVEL

While our measurement precision is not limited by the shot noise of the photodetection system, it is illuminating to understand how the shot-noise level would have appeared in our setting. The electric current through the photodiode is $I = \kappa e \mathcal{P} / h\nu$, where \mathcal{P} is the signal power, e is the electron charge magnitude, and κ is the quantum efficiency of the photodiode. $\kappa \simeq 0.8$ for the photodiodes we use. The current generated by shot noise is

$$I_{\text{SN}} = \sqrt{2eI \Delta f} = e \sqrt{\frac{2\kappa \mathcal{P}}{h\nu} \Delta f}. \quad (20)$$

Δf is the frequency range of the measurement. The signal in the experiment comes from difference in the current ΔI due to the geometric effects of the optical lever. For an inclination θ , the signal is

$$\Delta I = \kappa \frac{2e\theta \mathcal{P}}{h\nu NA}. \quad (21)$$

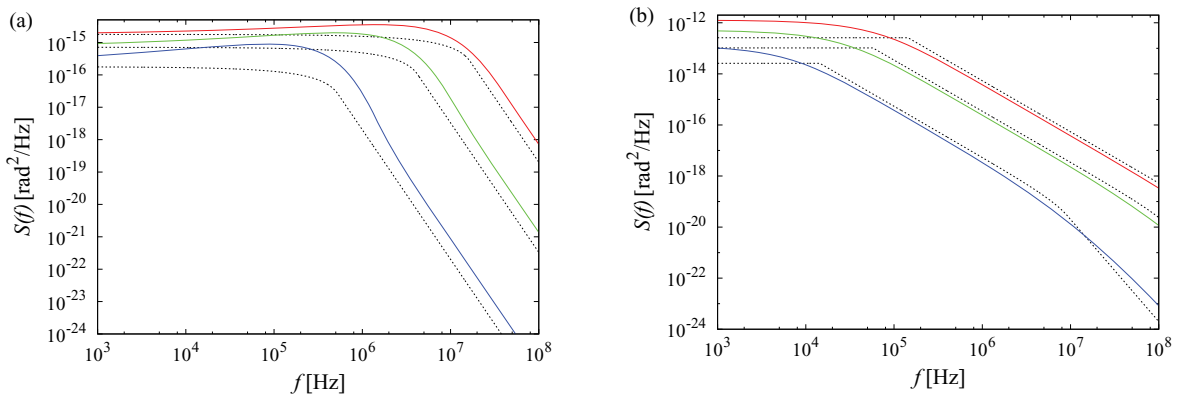


FIG. 4. (Color online) $S(f)$, the integrated spectra of surface fluctuations, computed numerically for (a) water and (b) oil with respect to f . The spectra are shown for $b = 0.85, 1.7, 7.1$ (μm^{-1}) [red (upper), green (middle), blue (lower) lines, respectively], along with their analytic approximations (black dashed). The spectra for smaller b have larger fluctuations across the spectrum.

The shot-noise level in our experiment is the size of the angular fluctuations θ_{SN}^2 corresponding to the shot-noise current. This is what appears in the measurements, had we *not* used the noise reduction through correlations described in Sec. V. θ_{SN}^2 can be obtained from $\Delta I \simeq I_{\text{SN}}$ to be

$$\theta_{\text{SN}}^2 \simeq \frac{\text{NA}^2 e}{2I} \Delta f. \quad (22)$$

Here, the current I is the photoelectric current collected by the dual photodiodes. θ_{SN}^2 is smaller for larger signals, which is natural. In addition, for larger numerical apertures, the beam spot is focused down to a smaller size so that the effect of the optical lever is smaller, hence the shot-noise effects are larger. In our experiment, $I \simeq 3 \mu\text{A}$ so that $\theta_{\text{SN}}^2 \simeq \text{NA}^2 \times 3 \times 10^{-14} \text{ rad}^2/\text{Hz}$. It is crucial to separate out the signal from this noise, using methods explained in the next section.

V. NOISE REDUCTION THROUGH CORRELATIONS

An essential feature of thermal fluctuations is that they are random. Since our objective is to directly measure the fluctuations under normal circumstances, the fluctuations are furthermore small. Even in ideally executed experiments, some random noise, such as shot noise, always exist. Therefore, to measure weak random signals, we need to separate out the random signal from the random noise. This is possible under rather general circumstances, as we now explain [13]. The principle behind this noise reduction is not limited to thermal fluctuations or optical measurements, but applies generally to the extraction of random signals from random noise. The conditions for its applicability will be discussed below.

A detector measurement $D_1 = S + N_1$ consists of the desired signal S and some noise N_1 , independent of S . Denoting Fourier transforms with tildes, the power spectrum obtained under simple averaging is

$$\langle |\tilde{D}_1|^2 \rangle = \langle |\tilde{S}|^2 \rangle + \langle |\tilde{N}_1|^2 \rangle. \quad (23)$$

Since the signal itself is random in nature, there is no way to distinguish the signal from the noise, so that the signal cannot be measured, unless the signal is larger than the noise, $\langle |\tilde{S}|^2 \rangle \gg \langle |\tilde{N}_1|^2 \rangle$. If we use only one measurement, this is an essential limitation.

To overcome this obstacle, we make another independent measurement of the same signal, $D_2 = S + N_2$, where N_2 denotes the noise for this measurement. Then,

$$\overline{\langle \tilde{D}_1 \tilde{D}_2 \rangle} \rightarrow \langle |\tilde{S}|^2 \rangle, \quad \mathcal{N} \rightarrow \infty, \quad (24)$$

eliminating the random noise N_1, N_2 . Here \mathcal{N} is the number of averagings. This result holds since the measurements D_1, D_2 are independent and the cross terms of decorrelated random observables (and their Fourier transforms) vanish under averaging. The relative error in this method is $\sim 1/\sqrt{\mathcal{N}}$, which arises from the statistical nature of the method. In principle, given enough averagings, we can suppress shot noise and other random noise effects to an arbitrarily small size.

The crucial requirements for our method to work is that multiple independent measurements can be made and that the signal is stable enough to withstand averagings. The independence of the measurements, or equivalently, the decorrelation of the noise in them is clearly crucial. As the

signal becomes weaker, stricter independence is required, which in practice can be quite delicate. For instance, cross talks can arise in electronic circuits, unless they are completely separated and electronic signals can affect each other through electromagnetic fields in the intervening space. These properties put practical limitations on the reduced noise level. While our method cannot be used for a one-time event, it can be used for any recurrent signal.

Specifically within our experiment, there exist five main sources of noise which need to be greatly reduced to achieve the desired sensitivity which is four orders of magnitude below the shot-noise level. First source is the shot noise within the photoelectric conversion processes. Second source is the amplification noise that arises mainly from thermal noise and noise within the semiconductor chips. Third source is the amplitude modulation (AM) noise of the laser beam. Fourth source is the frequency modulation (FM) noise of the laser beam. While the system may seem insensitive to this FM noise through the use of dual-element photodiodes, unwanted interference effects in the experimental setup have frequency-dependent response, leading to significant noise levels. Fifth source is the directional fluctuation of the laser beam. First two sources of noise arise within the photodetection system so that they can be eliminated by using duplicate dual-element photodetectors. The other three types of noise can be eliminated by using different laser sources. So our setup that uses laser sources with two wavelengths and two detector systems lead to two independent measurements which can easily be separated. Using the correlation of these measurements, all these types of noise can be removed, in theory as well as in practice. While it is also possible, in principle, to use a single laser with one wavelength for the measurements, more sophistication is necessary to obtain two independent measurements of the same signal.

Another possible approach to reducing the relative noise is to increase the signal strength. In our context, this would mean increasing the beam intensity. However, this is not always applicable, since a stronger beam will affect the sample. Even for simple liquid surfaces, it leads to more evaporation and can lead to less precise measurements. More generally, if we consider measuring the physics properties of biological materials, as required for medical applications [23], using a strong light source is often excluded. In surface light scattering experiments, heterodyne detection involving correlations of the signal and a reference signal has been used previously [24]. While in a different area, cross correlations have been used in dynamic light scattering (DLS) to study the properties of particles suspended in a liquid [25–27]. In DLS, cross correlations of scattered light from different paths are used to reduce contributions from multiple scattering and to study the properties of a single particle. In contrast, we use the cross correlations of independent measurements of the same signal from the same path to reduce the noise.

VI. EXPERIMENTAL RESULTS AND THEORY

In Fig. 5, we compare the experimentally measured spectra against the theory explained above for water, ethanol, and oil (Olympus immersion oil AX9602) with various beam sizes. We analyze the frequency range from a few hundred to

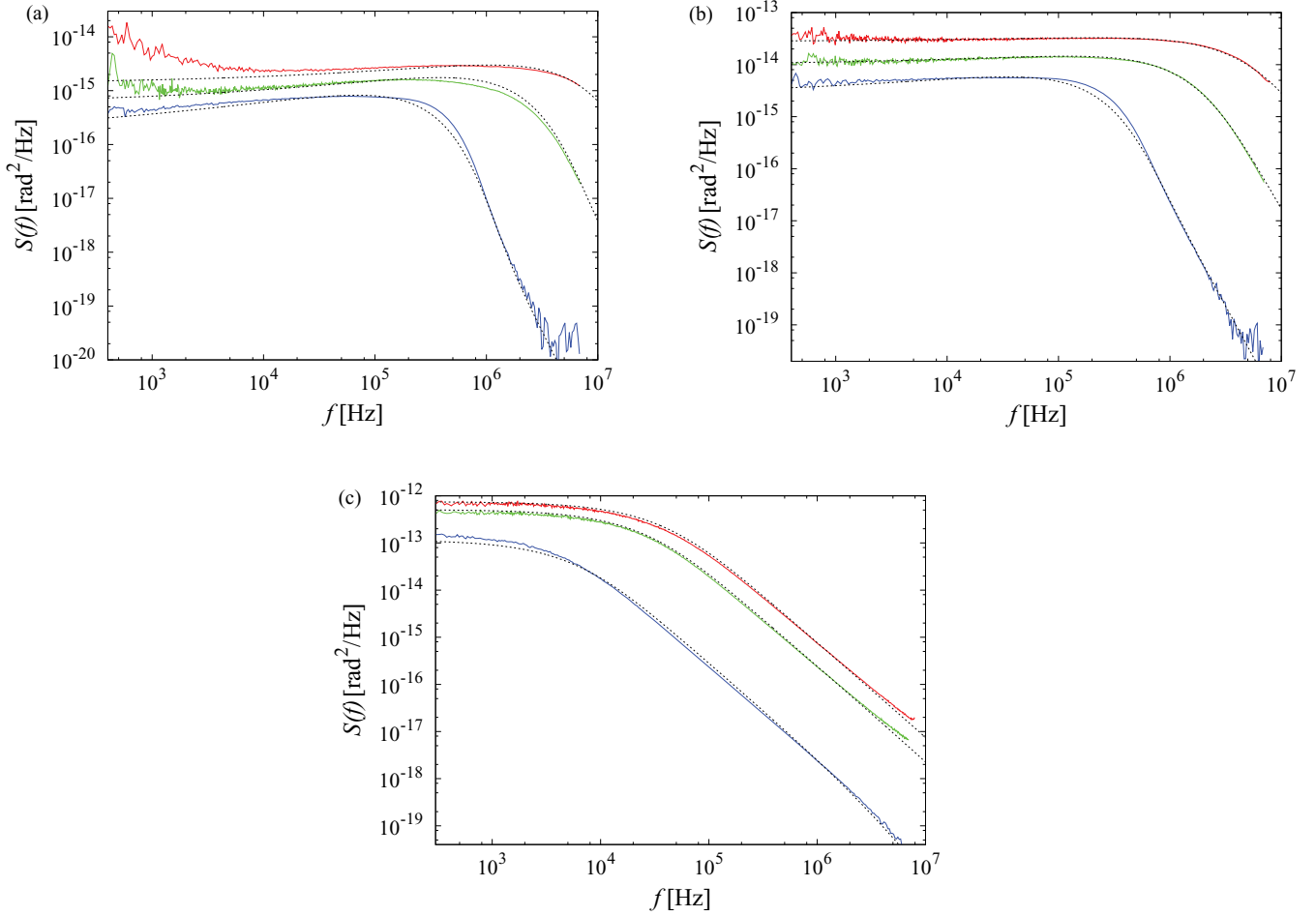


FIG. 5. (Color online) Experimentally observed fluctuation spectra for (a) water [$b = 0.92, 2.2, 8.1$ (μm)], (b) ethanol [$b = 0.64, 1.8, 6.7$ (μm)], and (c) oil [$b = 1.2, 1.8, 7.8$ (μm)]; red (upper), green (middle), blue (lower) lines from smaller to larger b . Respective theoretical spectra $S(f)$ are also shown (black dashed). The spectra for smaller b have larger fluctuations.

7×10^6 Hz. Due to the aforementioned cutoffs, the wavelengths of the surface waves we study range from μm to few mm. The fluid properties we used for water, ethanol, and oil are $\{\rho$ [kg/m^3], σ [kg/s^2], η [$\text{kg}/(\text{m} \cdot \text{s})$]\} = $(1.0 \times 10^3, 7.3 \times 10^{-2}, 1.0 \times 10^{-3})$, $(0.79 \times 10^3, 2.2 \times 10^{-2}, 1.1 \times 10^{-3})$, and $(0.92 \times 10^3, 3.0 \times 10^{-2}, 0.124)$, respectively. The agreement between the theoretical formula Eq. (11) and the experimental measurements is mostly quite satisfactory, including its beam size dependence. Going in the other direction, given a spectrum, we could have deduced the physical properties of the liquid. For instance, given ρ , which can usually be obtained independently, σ, η can be determined within 10% or so. There is some excess signal in the water surface fluctuations at low frequencies for small b [$b = 0.92 \mu\text{m}$ case in Fig. 5(a)], whose cause is discussed below. The rough features of the spectra can be understood from Eqs. (18) and (19); the spectrum behaves as $S(f) \sim \eta/(\sigma^2 b)$ at low frequencies. So, the spectral density of the fluctuations is largest for oil due to its high viscosity and smallest for water due to its large surface tension. The fluctuations are larger for smaller b . At high frequencies, as we decrease b , the effective cutoff for the wavelength decreases and fluctuations at larger frequencies become more apparent.

While the exact cause of the excess signal in the water surface fluctuation spectrum at low frequencies for $b = 0.92 \mu\text{m}$ is not certain, a plausible explanation is the following: Ideally, the experiment measures only inclination fluctuations of the surface. However, if there is an imperfection in the beam symmetry or in its alignment, the setup is weakly sensitive also to surface height fluctuations. This is especially true for larger NA (or equivalently smaller b), when the depth of field is shallow. The dimensionless ratio of the height fluctuation spectrum to the inclination spectrum has the dependence, $\langle |\tilde{a}_0(\omega)|^2 \rangle / (\langle |\tilde{a}_1(\omega)|^2 \rangle b^2) \sim \sigma / (\eta b f)$. $1/f$ dependence contributes to larger signal at lower frequencies and the ratio is larger for liquids with higher σ , such as water, and at small b . Therefore, a very weak sensitivity in the surface height fluctuations can give rise to the excess signal such as those seen in Fig. 5(a).

The shot-noise levels in the measurements are 3×10^{-15} , 1×10^{-15} , 7×10^{-17} (Hz^{-1}) for the beam diameters $b = 1, 2, 8$ (μm), as explained in Sec. IV. Therefore, we see that the noise reduction using signal correlations explained in the previous section is crucial for examining even the qualitative features of the spectra, since most, and in some cases all, of the spectra can be below shot-noise levels.

Some comments regarding the calibration of the measurements is in order. On the theoretical side, given the properties of the liquid and the beam diameter, there are *no* further parameters at all in the spectrum Eq. (11), which is specified completely. Experimentally, the frequency dependence of the spectrum can be measured precisely. Calibrating the overall magnitude of the measured spectrum is more difficult and this is done using a piezoelectrically driven mirror with a known oscillation amplitude. While this works well when b is large, for smaller b , the shallowness of the depth of field makes the calibration less accurate. Another complication is that the liquid in general evaporates during the measurement so that the beam defocuses. This, in effect, increases the beam diameter and can influence the spectral shape. This problem is clearly more acute for larger beam powers. A typical measurement of simple liquid surface fluctuations takes around 20 s and the beam power applied is 0.5 mW. Given the excellent agreement of the observed fluctuation spectra of simple liquid surfaces and theory, it might be reasonable to use thermal surface fluctuations of a specific liquid having well-known properties and a high boiling point to finely calibrate the system, when applying the measurements to more general samples.

In this work, we directly studied the spectra of thermal fluctuations for simple liquids, using surface light reflection methods. The spectra obtained are integrated over wavelengths and we have also investigated the dependence of the spectra on the beam diameter. In the process, we applied a novel general method for noise reduction, using the correlation of independent measurements of the same signal. The spectra obtained experimentally matches well with the theory,

whose approximate analytic behavior can be summarized rather simply. The derived analytic behavior elucidates the physics underlying the properties of the spectral functions, depending on the regime. Theoretically, the spectrum is uniquely determined by the physical properties of the liquid and the beam diameter. The agreement between the theoretical and the experimental results for liquids with quite different properties—for instance, water with strong surface tension, oil with high viscosity—over a wide frequency range and for various beam sizes provides a highly nontrivial check on the theory. Such detailed analysis of the spectra seems difficult in other methods, since the shot-noise level is high unless a stronger light is used, in which case the sample is affected. The measurement method is complementary to the surface fluctuation measurements for specific wavelengths, when applied to simple liquids. The method, especially when combined with the noise reduction method, has a broad range of applicability, especially since the required sample size, observation time, and power are small. The method can hence be also used for measuring fluctuation spectra of biological materials which can be affected by the probe light and physical properties of transient phenomena, such as those involving paint or epoxy [13].

ACKNOWLEDGMENT

K.A. was supported in part by the Grant-in-Aid for Scientific Research (Grant No. 20540279) from the Ministry of Education, Culture, Sports, Science and Technology of Japan.

-
- [1] M. von Schmoluchowski, *Ann. Physik* **25**, 205 (1908); L. Mandelstam, *ibid.* **41**, 609 (1913).
 - [2] D. Langevin, *Light Scattering by Liquid Surfaces and Complementary Techniques* (Marcel Dekker, New York, 1992).
 - [3] D. H. Vlad and J. V. Maher, *Phys. Rev. E* **59**, 476 (1999).
 - [4] P. Cicuta, A. Vailati, and M. Giglio, *Phys. Rev. E* **62**, 4920 (2000).
 - [5] J. A. Pojman *et al.*, *Langmuir* **22**, 2569 (2006).
 - [6] K. R. Mecke and S. Dietrich, *Phys. Rev. E* **59**, 6766 (1999); *J. Chem. Phys.* **123**, 204723 (2005).
 - [7] K. Sakai, H. Honda, and Y. Hiraoka, *Rev. Sci. Instrum.* **76**, 063908 (2005).
 - [8] Y. Ohmasa, T. Hoshino, R. Osada, and M. Yao, *Phys. Rev. E* **79**, 061601 (2009).
 - [9] K. Numata, M. Ando, K. Yamamoto, S. Otsuka, and K. Tsubono, *Phys. Rev. Lett.* **91**, 260602 (2003); E. D. Black *et al.*, *Phys. Lett. A* **328**, 1 (2004).
 - [10] H. J. Lauter, H. Godfrin, V. L. P. Frank, and P. Leiderer, *Phys. Rev. Lett.* **68**, 2484 (1992); A. Vailati and M. Giglio, *Nature (London)* **390**, 262 (1997).
 - [11] T. Mitsui, *Jpn. J. Appl. Phys.* **47**, 6563 (2008).
 - [12] A. Tay *et al.*, *Rev. Sci. Instrum.* **79**, 103107 (2008).
 - [13] T. Mitsui and K. Aoki, *Phys. Rev. E* **80**, 020602(R) (2009).
 - [14] R. V. Jones, *J. Sci. Instrum.* **38**, 37 (1961).
 - [15] R. H. Katyl and U. Ingard, *Phys. Rev. Lett.* **19**, 64 (1967).
 - [16] L. B. Shih, *Rev. Sci. Instrum.* **55**, 716 (1984).
 - [17] R. B. Dorshow, A. Hajiloo, and R. L. O. Swofford, *J. Appl. Phys.* **63**, 1265 (1988).
 - [18] S. Hard and R. D. Neuman, *J. Coll. Int. Sci* **115**, 73 (1987).
 - [19] D. Mizuno *et al.*, *Langmuir* **16**, 643 (2000).
 - [20] K. Sakai, P.-K. Choi, H. Tanaka, and K. Takagi, *Rev. Sci. Instrum.* **62**, 1192 (1991).
 - [21] V. G. Levich, *Physicochemical Hydrodynamics* (Prentice-Hall, Englewood Cliffs, 1962).
 - [22] M.-A. Bouchiat and J. Meunier, *J. de Phys.* **32**, 561 (1971).
 - [23] W. Denk and W. W. Webb, *Appl. Opt.* **29**, 2382 (1990).
 - [24] J. C. Earnshaw, *Appl. Opt.* **36**, 7583 (1997).
 - [25] G. D. J. Phillies, *J. Chem. Phys.* **74**, 260 (1981).
 - [26] G. D. J. Phillies, *Phys. Rev.* **24**, 1939 (1981).
 - [27] M. Drewel, J. Ahrens, and U. Podschus, *J. Opt. Soc. Am.* **7**, 206 (1990).